Catalysis Today 149 (2010) 111–116

Contents lists available at ScienceDirect

Catalysis Today

journal homepage: www.elsevier.com/locate/cattod

Influences of preparation methods of ZrO_2 support and treatment conditions of Cu/ZrO_2 catalysts on synthesis of methanol via CO hydrogenation

Yongge Bai [a,b], Dehua He [a,*], Shaohui Ge [a], Huimin Liu [a], Jinyao Liu [a], Wei Huang [b]

[a] Innovative Catalysis Program, Key Lab of Organic Optoelectronics & Molecular Engineering (MOE), Department of Chemistry, Tsinghua University, 1 Qinghua Yuan, Haidian, Beijing 100084, PR China

[b] Key Laboratory of Coal Science and Technology of Ministry of Education and Shanxi Province, Taiyuan University of Technology, Taiyuan 030024, PR China

ARTICLE INFO

Article history:
Available online 5 April 2009

Keywords:
Copper catalysts
Zirconia
Methanol
CO hydrogenation

ABSTRACT

ZrO_2 supports were prepared by different methods (conventional precipitation method, shortened as "CP", and alcogel/thermal treated with nitrogen method, shortened as "AN"), and Cu/ZrO_2 catalysts were prepared by impregnation method. The supports and catalysts were characterized by BET, XRD, TEM and TPR. The effects of the preparation methods of ZrO_2 supports and the treatment conditions (calcination and reduction temperatures) of the catalyst precursors on the texture structures of the supports and catalysts as well as on the catalytic performances of Cu/ZrO_2 in CO hydrogenation were investigated. The results showed that the support ZrO_2-AN had larger BET specific surface area, cumulative pore volume and average pore size than the support ZrO_2-CP. Cu/ZrO_2-AN catalysts showed higher CO hydrogenation activity and selectivity of oxygenates (C_1–C_4 alcohols and dimethyl ether) than Cu/ZrO_2-CP catalysts. Calcination and reduction temperatures of supports and catalyst precursors affected the catalytic performance of Cu/ZrO_2. The conversion of CO and the STY of oxygenates were 12.7% and 229 g/kg h, respectively, over Cu/ZrO_2-AN-550 at the conditions of 300 °C, 6 MPa.

1. Introduction

The catalytic conversion of syngas to methanol, DME (dimethyl ether) and higher alcohols (C_2–C_4 alcohols) is generally recognized as an important way to provide chemical stocks and clean fuel or fuel additives. Methanol is an important raw material in chemical industries, which can be used as the starting feedstock for C_1 chemistry. DME is considered to be an important chemical material and potential clean fuel substituting for LPG [1]. The most promising application of higher alcohols, especially isobutanol, is as an additive of blending stock for automotive fuel to meet the octane requirement for replacing MTBE (methyl t-butyl ether) [2]. Therefore, from the aspect of utilizing coal resources rationally, it is of significant importance to carry out researches on the synthesis of methanol, DME and higher alcohols.

ZrO_2, which is known to be an active isosynthesis (CO hydrogenation to iso-C_4 hydrocarbons) catalyst [3–6], has shown selectivity to isobutene in CO hydrogenation. Recently, it has been discovered that ZrO_2 also exhibits selectivity to isobutanol, however, at the same time, it suffers from low reactivity and harsh reaction conditions such as high temperature and high pressure. Cai et al. [7] have employed ZrO_2 modified by 2.0% K_2O as catalysts and obtained the results that under the reaction conditions of 420 °C, 10 MPa and 5000 h^{-1}, the space time yield (STP) of isobutanol was 3.99 mL/(L h), which accounted for 15.13 wt% of the products. Therefore, it is necessary to improve the activity of ZrO_2 and decrease the reaction temperatures. As a catalyst for methanol synthesis, Cu/ZrO_2 has been investigated to a great extent, including its preparation method [8,9], redox properties [10,11] and the disperse state of CuO [12,13]. However, as a catalyst for higher alcohol synthesis, Cu/ZrO_2 has not been reported in detail [14]. Considering the isosynthesis properties of ZrO_2 [15–17], in the present work, the effects of the preparation methods of ZrO_2 supports and the treatment conditions (calcination and reduction temperatures) of Cu/ZrO_2 catalysts on the catalytic performances of the catalysts in CO hydrogenation were investigated.

2. Experimental

2.1. Preparation of catalysts

All the chemicals used in present study are of analytical grade. ZrO_2 supports were prepared by two different methods, conventional precipitation method (denoted as CP method) and the method of drying and calcinating of $ZrO(OH)_2$ alcogel in N_2 (denoted as AN method) [18]. Firstly, $ZrO(NO_3)_2$ aqueous solution (0.17 M) was added dropwise into diluted NH_3 solution (2.5 wt%)

* Corresponding author. Tel.: +86 10 62773346; fax: +86 10 62773346.
E-mail address: hedeh@mail.tsinghua.edu.cn (D. He).

0920-5861/$ – see front matter © 2009 Elsevier B.V. All rights reserved.
doi:10.1016/j.cattod.2009.02.040

with vigorous stirring, which were continued for another 30 min after titration. Then the white precipitate of $ZrO(OH)_2$ was aged at room temperature for 10 h. Subsequently, the precipitate was filtered and washed thoroughly with deionized water till pH 7. $ZrO(OH)_2$ hydrogel was divided into two equal parts. One part of $ZrO(OH)_2$ hydrogel was dried at 110 °C for 10 h in air and then calcined at 550 °C for 5 h, yielding ZrO_2, which was denoted as ZrO_2-CP-550, where 550 represented the temperature of calcination (this preparation method was named as CP method). The other part was thoroughly washed with pure ethanol twice and the formed alcogel was dried at 110 °C for 10 h in a flowing N_2 and then further calcined at 550 °C for 5 h in a flowing N_2. The calcined sample was denoted as ZrO_2-AN-550. The samples prepared with the same procedure as ZrO_2-AN-550 but calcined at 400 °C and 700 °C were denoted as ZrO_2-AN-400 and ZrO_2-AN-700, respectively. Cu/ZrO_2 catalysts were obtained by impregnating ZrO_2-CP and ZrO_2-AN with $Cu(NO_3)_2$ aqueous solution for 24 h, and then dried at 110 °C for 10 h in air and calcined at 350 °C for 3 h. The prepared CuO/ZrO_2 precursors were denoted as CuO/ZrO_2-AN-T1-T2 and CuO/ZrO_2-CP-T1-T2, in which T1 represented the calcination temperatures of ZrO_2-AN or ZrO_2-CP and T2 represented the calcination temperatures of CuO/ZrO_2.

2.2. Characterization of catalysts

N_2 adsorption isotherms were measured at 77 K using an ASAP-2010C gas adsorption analyzer (Micromeritics Corp). X-ray diffraction (XRD) measurements were performed on a Bruker D8 advance X-ray diffractometer, using Ni filtered Cu radiation at room temperature and instrumental settings of 40 kV and 40 mA. The average size of crystal could be measured by X-ray line broadening analysis (XLBA) using the well-known Debye–Scherrer equation [19]. Transmission electron microscope (TEM) measurements were carried out on JEOL-2010 to investigate the morphology and microstructure of samples.

H_2-temperature programmed reduction (H_2-TPR) was carried out on a homemade analysis system. The sample (100 mg) was first pretreated in a flow of Ar at 250 °C for 2 h and then cooled down to room temperature. Subsequently, under a flowing of 5% H_2/Ar mixture (30 ml/min), the sample was again heated from 20 °C to 700 °C at a heating rate of 10 °C/min.

2.3. Catalyst testing

The purities of H_2 and CO used in the study are 99.999% and 99.9%, respectively. CO hydrogenation was carried out in a specially designed high-pressure flow fixed-bed reactor. It was a quartz-lined stainless-steel tubular reactor in which the quartz line (10 I.D.) was tightly fixed in a stainless-steel tube. The catalyst (0.5 ml, 20–40 mesh) was packed in the reactor. Before the reaction was conducted, the catalyst was reduced at a certain temperature for 2 h in 20% H_2/N_2. Then the temperature was adjusted to reaction temperature and syngas (H_2/CO = 1:1) was introduced into the reactor. Both gaseous and liquid products were analyzed by gas chromatographs. H_2, CO, CO_2 and C_1–C_5 hydrocarbons were determined on-line by thermal conductivity detector (TCD) with a TDX-01 column, and oxygenates were analyzed off-line by flame ionization detector (FID) with an OV-17 capillary column.

3. Results and discussion

3.1. Influence of preparation methods of ZrO_2 supports on textural properties and catalytic performance

The adsorption and desorption isotherms of ZrO_2-AN, ZrO_2-CP, CuO/ZrO_2-AN and CuO/ZrO_2-AN are given in Fig. 1 and the BJH pore

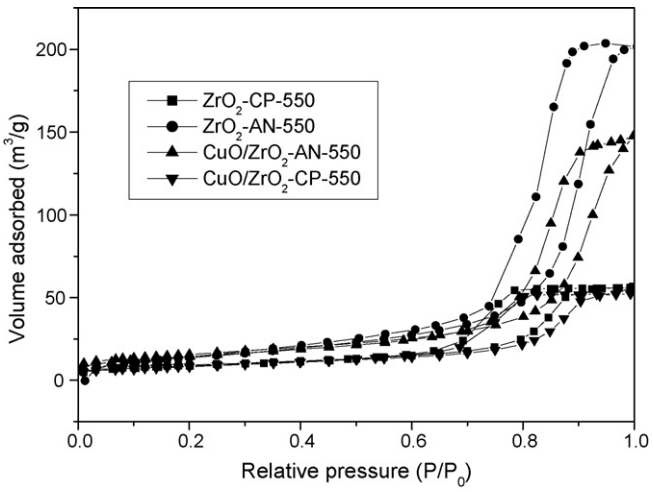

Fig. 1. N_2 adsorption–desorption isotherms of samples.

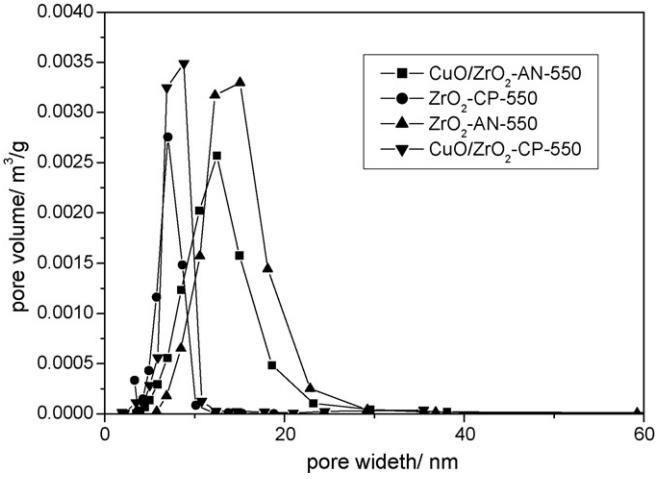

Fig. 2. BJH pore size distributions of samples.

size distributions of these samples are given in Fig. 2. Obviously, these samples showed the same type of adsorption isotherms (type IV) and hysteresis loops [20]. However, compared with ZrO_2-CP-550, ZrO_2-AN-550 had higher adsorption capacity and larger cumulative pore volume. In addition, the pore size distributions of ZrO_2-AN-550 were in the range of 7–35 nm, while those of ZrO_2-CP-550 were in the range of 4–11 nm. After the loading of CuO over ZrO_2-AN-550, the adsorption capacity and the cumulative pore volume decreased, and the pore size distributions shifted to a lower range.

The information about the textural structures of ZrO_2-AN, ZrO_2-CP, Cu/ZrO_2-AN and Cu/ZrO_2-CP is presented in Table 1. The specific surface area of ZrO_2-AN-550 was 61 m^2/g, which was almost twice that of ZrO_2-CP-550. Moreover, the cumulative pore volume and the average pore size of ZrO_2-AN-550 were three and

Table 1
Effects of preparation methods of ZrO_2 on texture structure of ZrO_2.

Sample	S_{BET} ($m^2\ g^{-1}$)	Cumulative pore volume ($cm^3\ g^{-1}$)	Average pore size (nm)	Crystal size of ZrO_2 (nm)[a]
ZrO_2-AN-550	61	0.28	14	15
ZrO_2-CP-550	33	0.09	7	18
CuO/ZrO_2-AN-550	56	0.21	13	14
CuO/ZrO_2-CP-550	31	0.16	7	–

[a] Calculated from the X-ray line broadening analysis.

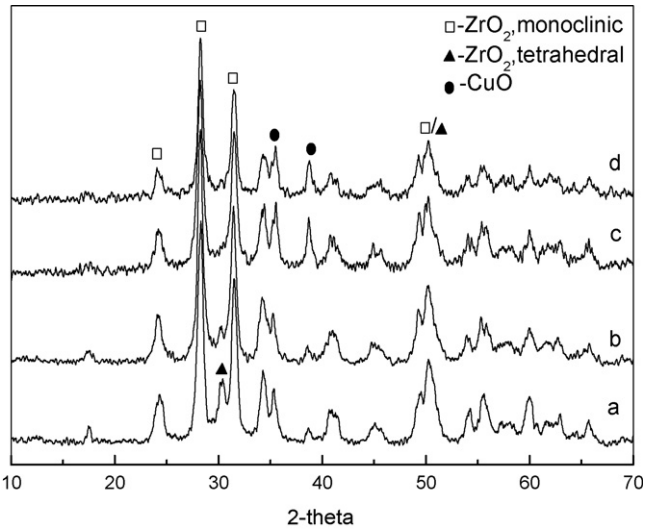

Fig. 3. XRD patterns of ZrO_2 and CuO/ZrO_2.

two times as large as those of ZrO_2-CP-550, respectively. By comparing the data for ZrO_2-AN and CuO/ZrO_2-AN, it can be seen that loading of CuO over ZrO_2-AN brought about slight decreases in the specific surface area, cumulative pore volume and average pore size.

The crystal phases of ZrO_2-AN, ZrO_2-CP, CuO/ZrO_2-AN and CuO/ZrO_2-CP were determined by XRD, and the XRD patterns of these samples are displayed in Fig. 3. In both ZrO_2-AN-550 and ZrO_2-CP-550, there were dominating monoclinic ZrO_2 phase together with a trace tetragonal ZrO_2 phase. Nevertheless, the diffraction peaks of ZrO_2 over ZrO_2-CP-550 were sharper, indicating the larger crystal sizes of ZrO_2-CP-550 (the crystal sizes of ZrO_2-CP-550 and ZrO_2-AN-550, which were calculated by Debye–Scherrer equation, were 18 nm and 15 nm, respectively, as can be seen in Table 1). The peaks of CuO appeared and with similar intensities over both supports after the loading of ZrO_2-CP-550 or ZrO_2-AN-550 with CuO, however, no peaks of monoclinic ZrO_2 were detected.

From the TEM studies shown in Fig. 4, it could be seen that the size distribution of ZrO_2-CP-550 particles was wide (about 16–24 nm), indicating the occurrence of agglomeration, while the sizes of ZrO_2-AN-550, by contrast, were uniform and relatively small (about 12–15 nm). The sizes determined by TEM were in agreement with the results obtained by XRD.

From Table 2, where the results of CO hydrogenation over ZrO_2-AN, Cu/ZrO_2-AN and Cu/ZrO_2-CP are listed, it could be seen that the activity over ZrO_2-AN-550 support was rather low at 260 °C. CO conversion was just 0.5%, with 19.7 g/kg h oxygenates and 24.4 wt% dimethyl ether and 75.6 wt% methanol being produced. CO conversion, the selectivity to oxygenates and the STY of oxygenates over 9.1%Cu/ZrO_2-AN-550 were higher than those over 9.1%Cu/ZrO_2-CP-550. The STY of oxygenates over 9.1%Cu/ZrO_2-CP-550 was only 80.7 g/kg h and with little isobutanol produced, while the STY of oxygenates over 9.1%Cu/ZrO_2-AN-550 was 229.0 g/kg h with 1.4 wt% of isobutanol. The differences in the catalytic performance between Cu/ZrO_2-AN and Cu/ZrO_2-CP may be related with the specific surface area of ZrO_2 and the disperse state of Cu. The larger specific surface area of ZrO_2-AN-550 provided more contact surfaces between ZrO_2 and the active copper species, which was benefit for the formation of active centers and then the improvement in catalytic activity.

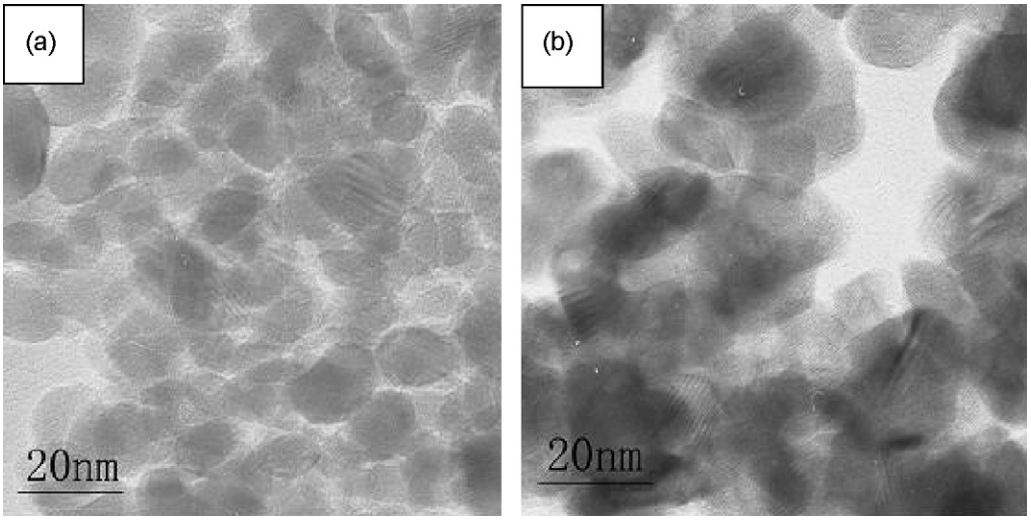

Fig. 4. TEM images of ZrO_2-AN and ZrO_2-CP: (a) ZrO_2-AN-550; (b) ZrO_2-CP-550.

Table 2
Effects of preparation methods on catalytic performances of 9.1%Cu/ZrO_2[a].

Catalyst	Conv.	Selectivity (%)			STY ($g\ kg^{-1}\ h^{-1}$)[d]	Distribution of oxygenates (wt%)			
	CO (%)	Oxy[b]	CH[c]	CO_2		DME	CH_3OH	C_2H_5OH	i-C_4H_9OH
ZrO_2-AN-550	0.5	100	Tr	Tr	19.7	24.4	75.6	Tr	Tr
Cu/ZrO_2-CP-550	8.7	26.8	31.9	41.3	80.7	17.5	82.3	0.2	Tr
Cu/ZrO_2-AN-550	12.7	41.3	23.0	35.7	229.0	11.8	86.4	0.5	1.4

[a] Reaction conditions: $H_2/CO = 2$, 300 °C, 6 MPa, 10,000 h^{-1}; reduction conditions: $V_{N_2}/V_{H_2} = 4/1$, 260 °C, 2 h.
[b] Oxy, oxygenates.
[c] HC, hydrocarbons.
[d] STY: space time yield of total oxygenates.

Table 3
Effects of calcination temperatures on texture structure of ZrO_2 and 9.1%Cu/ZrO_2.

No.	Sample	Calcination temp. (°C)		S_{BET} ($m^2\ g^{-1}$)	Cumulative pore volume ($cm^3\ g^{-1}$)	Average pore size (nm)	Crystal size of ZrO_2 (nm)[a]	
		Support	Catalyst				ZrO_2	CuO
1	ZrO_2-AN-400	400	–	160	0.31	6	–	–
2	ZrO_2-AN-550	550	–	61	0.28	14	15	–
3	ZrO_2-AN-700	700	–	30	0.15	16	25	–
4	Cu/ZrO_2-AN	400	350	139	0.27	6	–	–
5	Cu/ZrO_2-AN	550	350	56	0.21	13	14	15
6	Cu/ZrO_2-AN	700	350	28	0.13	16	23	19
7	Cu/ZrO_2-AN	550	550	60	0.20	11	13	–

[a] Calculated from the X-ray line broadening analysis.

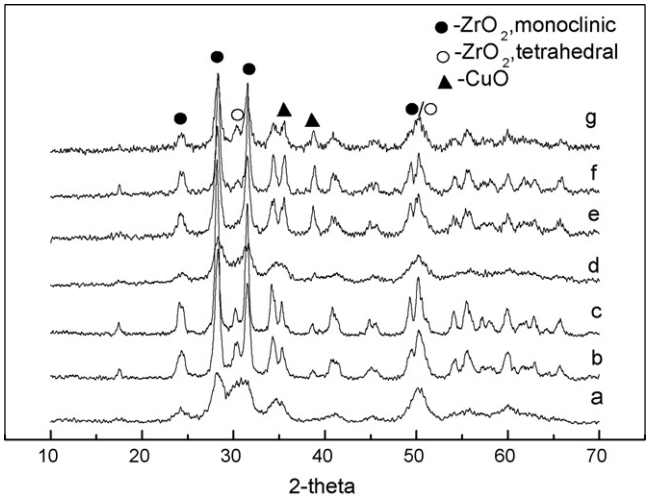

Fig. 5. XRD patterns of ZrO_2 and Cu/ZrO_2 samples calcined at different temperatures: (a) ZrO_2-AN-400; (b) ZrO_2-AN-550; (c) ZrO_2-AN-700; (d) 9.1%Cu/ZrO_2-AN-400-350; (e) 9.1%Cu/ZrO_2-AN-550-350; (f) 9.1%Cu/ZrO_2-AN-700-350; (g) 9.1%Cu/ZrO_2-AN-550-550.

3.2. Effects of treatment conditions on properties and catalytic performance of Cu/ZrO_2

As has been stated, ZrO_2-AN had larger specific surface area and then higher catalytic activity than ZrO_2-CP. For this reason, ZrO_2-AN was selected for further investigation, and the effects of calcination temperatures were investigated first. Table 3 lists several textural properties of ZrO_2-AN and Cu/ZrO_2-AN calcined at different temperatures. Nos. 1–3 revealed that, with an increase in the calcination temperature of ZrO_2-AN, its specific surface area and cumulative pore volume lowered, and its particle sizes and average pore sizes enlarged. The large surface area of ZrO_2-AN calcined at 400 °C (160 m^2/g) may result from the incomplete formation of crystal structure and less sintering due to the low calcination temperature (400 °C). After the loading of Cu on ZrO_2-AN and calcining at different temperatures, the specific surface area and cumulative pore volume decreased (shown in Table 3, Nos. 4–6). Compared with Cu/ZrO_2-AN-550-350, Cu/ZrO_2-AN-550-550 had larger specific surface area and smaller pore size and cumulative pore volume (Table 3, Nos. 5 and 7).

The XRD patterns of ZrO_2-AN and Cu/ZrO_2-AN calcined at different temperatures are shown in Fig. 5. The diffraction peaks of ZrO_2 calcined at 400 °C were weak and wide (as can be seen in Fig. 5a), indicating the incomplete formation of monoclinic ZrO_2 and the existence of amorphous ZrO_2. After the impregnation of ZrO_2-AN-400 with $Cu(NO_3)_2$ aqueous solution and then calcination at 350 °C, no diffraction peaks of CuO were detected (shown in Fig. 5d), implying that CuO was well-dispersed over ZrO_2-AN-400 and no bulk phase CuO was formed. This might be related with the larger specific surface area of ZrO_2-AN-400, which was 160 m^2/g. On the contrary, after the impregnation of monoclinic phase ZrO_2-AN-550 with $Cu(NO_3)_2$ aqueous solution, the peaks of CuO were detected. Increasing the calcination temperature from 550 °C to 700 °C made the peaks of monoclinic ZrO_2 and CuO sharpened, suggesting the growth of crystal sizes of ZrO_2 and the decrease in specific surface area (listed in Table 3). From XRD characterization, the particle size of CuO over ZrO_2-AN-700 was 19 nm, while that over ZrO_2-AN-550 was 15 nm. Compared with the catalyst precursor Cu/ZrO_2-AN calcined at 350 °C, the peaks of CuO over the catalyst precursor Cu/ZrO_2-AN calcined at 550 °C were weakened. The reason might be that the strong interactions between ZrO_2 and CuO at high temperature led to well dispersion of CuO over ZrO_2 [21,22].

The TEM images of ZrO_2-AN supports calcined at different temperatures are shown in Fig. 6. The growth of ZrO_2 particles could be observed with the increase in calcination temperatures, which was obvious at 700 °C. The average sizes of ZrO_2 particles calcined at 400 °C, 550 °C, and 700 °C were 11–13 nm, 12–15 nm, and 20–23 nm, respectively, which were consistent with the results obtained by XRD.

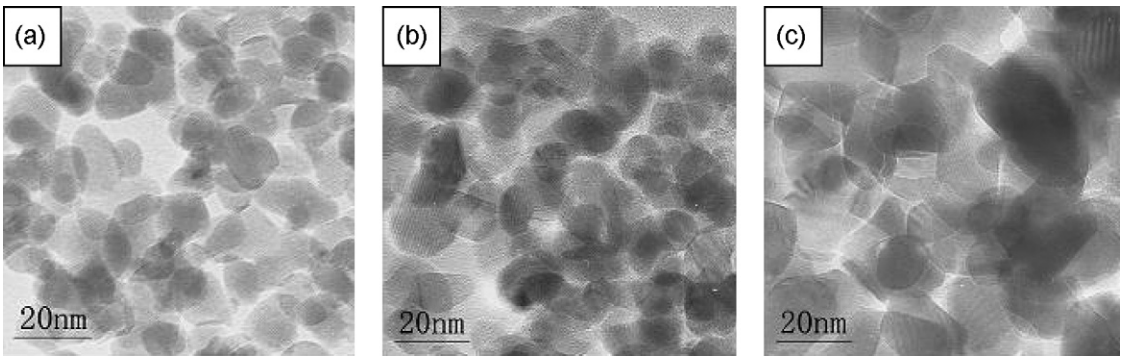

Fig. 6. TEM images of ZrO_2-AN calcinated at different temperatures: (a) ZrO_2-AN-400; (b) ZrO_2-AN-550; (c) ZrO_2-AN-700.

Table 4
Effects of calcination temperatures of ZrO_2 on catalytic performances of 9.1%Cu/ZrO_2[a].

Temperature (°C)	Conv	Selectivity (%)			STY (g kg^{-1} h^{-1})[d]	Distribution of oxygenates (wt%)			
	CO (%)	Oxy[b]	CH[c]	CO_2		DME	CH_3OH	C_2H_5OH	i-C_4H_9OH
400	13.8	36.8	30.8	32.4	232.4	23.3	75.2	0.5	1.0
550	12.7	41.3	23.0	35.7	229.0	11.8	86.4	0.5	1.4
700	5.5	70.6	29.4	0	144.9	4.3	93.8	1.1	0.8

[a] Reaction conditions: $H_2/CO = 2$, 300 °C, 6 MPa, 10,000 h^{-1}; reduction conditions: $V_{N_2}/V_{H_2} = 4/1$, 260 °C, 2 h.
[b] Oxy, oxygenates.
[c] HC, hydrocarbons.
[d] STY: space time yield of total oxygenates.

Table 5
Effects of calcination temperatures of CuO/ZrO_2 on catalytic performances of 9.1%Cu/ZrO_2[a].

Temperature (°C)	Conv	Selectivity (%)			STY (g kg^{-1} h^{-1})[d]	Distribution of oxygenates (wt%)			
	CO (%)	Oxy[b]	CH[c]	CO_2		DME	CH_3OH	C_2H_5OH	i-C_4H_9OH
350	12.7	41.3	23.0	35.7	229.0	11.8	86.4	0.5	1.4
550	1.3	35.2	25.5	39.3	162.4	14.1	84.0	0.7	1.2

[a] Reaction conditions: $H_2/CO = 2$, 300 °C, 6 MPa, 10,000 h^{-1}; reduction conditions: $V_{N_2}/V_{H_2} = 4/1$, 260 °C, 2 h.
[b] Oxy, oxygenates.
[c] HC, hydrocarbons.
[d] STY: space time yield of total oxygenates.

The influences of calcination temperatures of support ZrO_2-AN on the catalytic performance of CO hydrogenation were investigated and the results are listed in Table 4. It revealed that calcination temperature had little effect on CO conversion and STY of oxygenates when it was within the range of 400–550 °C. However, the results were quite different when the calcination temperature of ZrO_2-AN was raised from 550 °C to 700 °C. CO conversion decreased from 12.7% to 5.5%, STY of oxygenates decreased from 229.0 g/kg h to 144.9 g/kg h, and the selectivity to oxygenates, especially methanol, was improved. The percentage of isobutanol in oxygenate products reached up to 1.4% when ZrO_2-AN-550 was used as support. The differences in catalytic performance due to calcination temperature might be related with the disperse state of CuO over ZrO_2 surface. It has been reported that the highly dispersed Cu is the active center of Cu/ZrO_2 catalyst [8]. The results mentioned above illustrated that the supports calcined at higher temperatures had smaller specific surface area, which is not favorable for the dispersion of Cu. Zhou et al. found that excessive amount of CuO loaded on the surface of supports would cover the active copper species and then decrease the catalytic performance [10].

The effects of calcination temperatures of catalyst precursors Cu/ZrO_2-AN have been investigated and the results are summar-

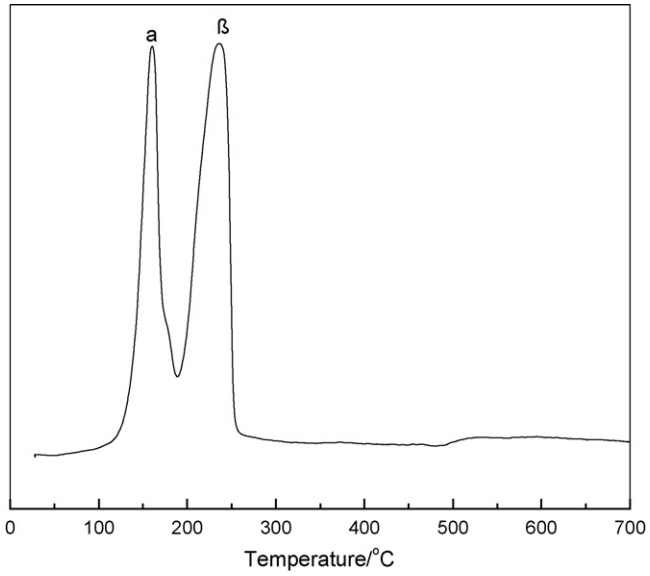

Fig. 7. TPR profile of CuO/ZrO_2-AN-550.

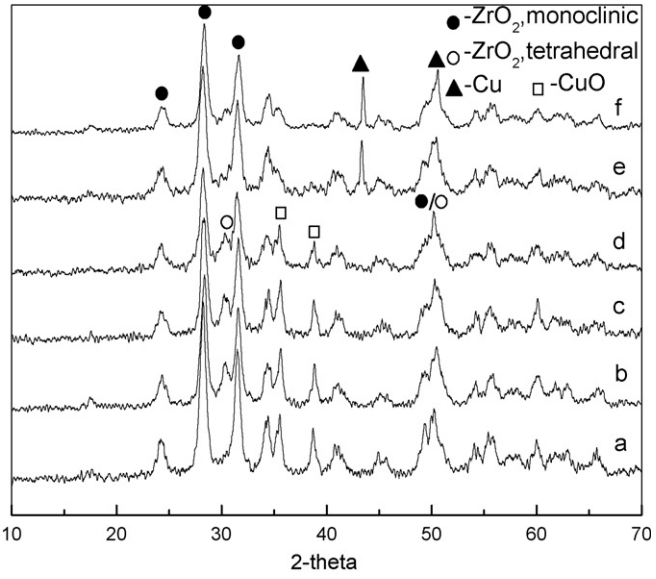

Fig. 8. XRD patterns of 9.1%Cu/ZrO_2 before and after reduction or reaction: (a) before reduction; (b) reduced at 260 °C for 2 h; (c) reduced at 350 °C for 2 h; (d) reduced at 450 °C for 10 h; (e) reacted at 300 °C; (f) reacted at 350 °C.

Table 6
Particle sizes of ZrO_2 and CuO in CuO/ZrO_2 reduced and reacted at different temperatures.

Sample	Reduction T (°C)	Reaction T (°C)	Crystal size of ZrO_2 (nm)[a]		
			ZrO_2	Cu	CuO
Cu/ZrO_2-AN-550-350	260	–	14	–	17
Cu/ZrO_2-AN-550-350	350	–	14	–	19
Cu/ZrO_2-AN-550-350	450	–	14	–	15
Cu/ZrO_2-AN-550-350	260	300	12	65	–
Cu/ZrO_2-AN-550-350	260	350	14	77	–

[a] Calculated from the X-ray line broadening analysis.

Table 7
Effects of reduction temperatures on catalytic performances of 9.1%Cu/ZrO_2[a].

Temperature (°C)	Conv	Selectivity (%)			STY (g kg^{-1} h^{-1})[d]	Distribution of oxygenates (wt%)			
	CO (%)	Oxy[b]	CH[c]	CO_2		DME	CH_3OH	C_2H_5OH	i-C_4H_9OH
260	12.7	41.3	23.0	35.7	229.0	11.8	86.4	0.5	1.4
350	10.8	39.9	33.3	26.8	165.3	15.6	82.6	0.6	1.2
450	8.8	46.6	23.8	29.6	162.1	16.3	82.6	0.5	0.5

[a] Reaction conditions: $H_2/CO = 2$, 300 °C, 6 MPa, 10,000 h^{-1}; reduction conditions: $V_{N_2}/V_{H_2} = 4/1$, 2 h.
[b] Oxy: oxygenates.
[c] HC: hydrocarbons
[d] STY: space time yield of total oxygenates.

ized in Table 5. Nearly the same conversion of CO was obtained over Cu/ZrO_2-AN-550-550 and Cu/ZrO_2-AN-550-350. However, the selectivity and STY of oxygenates were lower over Cu/ZrO_2-AN-550-550, which were 35.2% and 162.4 g/kg h, respectively, while they were 41.3% and 229.0 g/kg h, respectively over Cu/ZrO_2-AN-550-350. The differences could be attributed to the interactions between Cu and supports. Zhou et al. had investigated the effects of calcination temperatures on the active copper species loaded on γ-Al_2O_3, and found that high temperature led to the strong interactions between the active copper species and γ-Al_2O_3, forming $CuAl_2O_4$, which decreased its catalytic activity [10].

3.3. Effects of reduction temperatures of CuO/ZrO_2 on textural structures and catalytic performance

Reduction temperature plays a role in determining particle size and the disperse state of active component of catalysts. TPR characterization is also employed for discovering the optimal reduction temperature. The TPR result of 4.8% Cu/ZrO_2-AN is shown in Fig. 7. It can be seen that two reduction peaks were observed at 160 °C and 237 °C, designated as α and β. These two peaks were also reported in other studies and were interpreted to correspond with the reduction of highly dispersed CuO (peak α) and CuO crystalline in the cavities of ZrO_2 (peak β). The strong interactions between CuO in the cavities and ZrO_2 made it more difficult to be reduced [12,23].

The XRD results of Cu/ZrO_2-AN-550-350 reduced at different temperatures are shown in Fig. 8. It can be seen that, over the reduced catalysts, the crystallines of ZrO_2 and CuO were detected, however, the crystalline of Cu was not. Perhaps one reason is that the highly dispersed CuO was reduced to nanosized Cu instead of bulk phase Cu. The other reason might be that the nanosized Cu had been reoxidized to CuO when it contacted with air [24], since it has been reported that Cu of small particles was easily to be oxidized [18,25,26]. Moreover, the dominating phases of Cu/ZrO_2-AN-550, which was reduced at 260 °C and then reacted at 300 °C and 350 °C, respectively, were ZrO_2 and Cu, without CuO crystalline being detected (as shown in Fig. 8e and f). And the peaks for Cu sharpened with the increase in reaction temperature, which might be explained by the sintering of Cu at higher temperatures.

The results in Table 6 shows that the crystal size of Cu increased from 65 nm to 77 nm when reaction temperature was raised from 300 °C to 350 °C, however, no apparent differences in CuO particle sizes were observed with the variations in reduction temperature. The particle sizes of ZrO_2 were not affected by the reduction and reaction process within the temperature range adopted in this study.

The catalytic performance of 9.1%Cu/ZrO_2-AN-550 was investigated at different temperatures and the results are shown in Table 7. It can be seen that raising the reduction temperature of the catalyst lead to a decrease in CO conversion while keeping the selectivity to oxygenates unchanged. Over the catalyst calcined at high temperatures (350–450 °C), STY of oxygenates and selectivity to isobutanol decreased, while selectivity to DME increased.

4. Conclusions

Compared with ZrO_2-CP, ZrO_2-AN had larger specific surface area, cumulative pore volume and average pore size and showed relatively high CO conversion, STY of oxygenates and selectivity to isobutanol. Calcination temperatures of ZrO_2 support and Cu/ZrO_2 catalyst precursors affected their textural structure and catalytic performance. With the increase in calcination temperatures of ZrO_2, its specific surface area decreased, which led to the decrease in CO conversion and STY of oxygenates. Therefore, 550 °C was the suitable calcination temperature for ZrO_2. On increasing calcination temperatures of catalyst precursors, STY of oxygenates decreased. 350 °C was the suitable calcination temperature for catalyst precursors. The catalytic performance of Cu/ZrO_2 was also related with its reduction temperature. Too high reduction temperatures (>300 °C) resulted in the growth of Cu particles and then the decrease in catalytic performance.

Acknowledgments

This work was supported by National Natural Science Foundation of China (Grant No: 20590362) and Ministry of Science and Technology of China (Grant No: 2007AA05Z332).

References

[1] Y.S. Tan, H.J. Xie, H.T. Cui, Y.Z. Han, B. Zhong, Catal. Today 104 (2005) 25.
[2] R.G. Herman, Catal. Today 55 (2000) 233.
[3] T. Maehashi, K. Maruya, K. Domen, K. Aika, T. Onishi, Chem. Lett. 5 (1984) 747.
[4] C.L. Su, J.R. Li, D.H. He, Z.X. Cheng, Q.M. Zhu, Appl. Catal. A 202 (2000) 81.
[5] R. Raudaskoski, M.V. Niemela, R.L. Keiski, Top. Catal. 45 (2007) 57.
[6] W. Khaodee, B. Jongsomjit, S. Assabumrungrat, P. Praserthdam, S. Goto, Catal. Commun. 8 (2007) 548.
[7] Y.N. Cai, Y.Q. Niu, Z.H. Chen, B. Zhong, S.Y. Peng, J. Fuel Chem. Technol. 24 (1996) 11.
[8] J.Y. Liu, J.L. Shi, D.H. He, Q.J. Zhang, X.H. Wu, Y. Liang, Q.M. Zhu, Appl. Catal. A 218 (2001) 113.
[9] F. Arena, K. Barbera, G. Italiano, G. Bonura, L. Spadaro, F. Frusteri, J. Catal. 249 (2007) 185.
[10] R.X. Zhou, X.Y. Jiang, J.X. Mao, X.M. Zheng, Appl. Catal. A 162 (1997) 213.
[11] T.J. Keskitalo, M.K. VeringaNiemela, A.O.I. Krause, Langmuir 23 (2007) 7612.
[12] R.X. Zhou, X.Y. Jiang, G.L. Lee, X.M. Zheng, Chemical Research in Chinese Universities, 18 (1997) 1854.
[13] L.C. Wang, Q. Liu, M. Chen, Y.M. Liu, Y. Cao, H.Y. He, K.N. Fan, J. Phys. Chem. C 111 (2007) 16549.
[14] K.A. Pokrovski, A.T. Bell, J. Catal. 241 (2006) 276.
[15] Y.W. Li, D.H. He, Q.M. Zhu, X. Zhang, B.Q. Xu, J. Catal. 221 (2004) 584.
[16] Y.W. Li, D.H. He, Q.M. Zhu, B.Q. Xu, Appl. Catal. A 319 (2007) 119.
[17] Y.W. Li, D.H. He, S.H. Ge, R.J. Zhang, Q.M. Zhu, Appl. Catal. B 80 (2008) 72.
[19] B.D. Cullity, Elements of X-ray Diffraction, Addison-Wesley, Morris Cohen Press, 1978, p. 285.
[18] B.Q. Xu, J.M. Wei, J. Zhang, Q.M. Zhu, China Patent, CN 1260324 (2000).
[20] K.S.W. Sing, D.H. Everett, R.A.W. Hual, Pure Appl. Chem. 57 (1985) 603.
[21] Y.C. Xie, R.F. Yang, Y.J. Liu, Y.Q. Tang, Sci. China (Chem.) 8 (1992) 673.
[22] Y.C. Xei, Y.Q. Tang, Adv. Catal. 37 (1990) 1.
[23] M.G. Sanchez, J.L. Gazquez, J. Catal. 104 (1987) 120.
[24] K.V.R. Chary, G.V. Sagar, C.S. Srikanth, V.V.J. Rao, Phys. Chem. B 111 (2007) 543.
[25] M. Turco, G. Bagnasco, C. Cammarano, P. Senese, U. Costantino, M. Sisani, Appl. Catal. B 77 (2007) 46.
[26] M.F. Luo, Y.P. Song, J.Q. Lu, X.Y. Wang, Z.Y. Pu, J. Phys. Chem. C 111 (2007) 12686.